Published in final edited form as:

Connect Tissue Res. 2017 ; 58(3-4): 329–341. doi:10.1080/03008207.2016.1267152.

Fiber Development and Matrix Production in Tissue Engineered Menisci using Bovine Mesenchymal Stem Cells and Fibrochondrocytes

Mary Clare McCorry[1] and **Lawrence J. Bonassar, PhD**[1,2,*]

[1]Meinig of Biomedical Engineering, Cornell University, Ithaca, NY

[2]Sibley School of Mechanical and Aerospace Engineering, Cornell University, Ithaca, NY

Abstract

Mesenchymal stem cells (MSCs) have been investigated with promising results for meniscus healing and tissue engineering. While MSCs are known to contribute to ECM production, less is known about how MSCs produce and align large organized fibers for application to tissue engineering the meniscus. The goal of this study was to investigate the capability of MSCs to produce and organize extracellular matrix molecules compared to meniscal fibrochondrocytes (FCCs). Bovine FCCs and MSCs were encapsulated in an anatomically accurate collagen meniscus using mono-culture and co-culture of each cell type. Each meniscus was mechanically anchored at the horns to mimic the physiological fixation by the meniscal entheses. Mechanical fixation generates a static mechanical boundary condition previously shown to induce formation of oriented fiber by FCCs. Samples were cultured for 4 weeks and then evaluated for biochemical composition and fiber development. MSCs increased the GAG and collagen production in both co-culture and mono-culture groups compared to FCC mono-culture. Collagen organization was greatest in the FCC mono-culture group. While MSCs had increased matrix production they lacked the fiber organization capabilities of FCCs. This study suggests that GAG production and fiber formation are linked. Co-culture can be used as a means of balancing the synthetic properties of MSCs and the matrix remodeling capabilities of FCCs for tissue engineering applications.

Keywords

Mesenchymal Stem Cell; Collagen; Fiber; Meniscus; Tissue Engineering

Introduction

The meniscus is a fibrocartilaginous tissue comprised of a complex network of fibers with distributed glycosaminoglycans (GAGs) that collectively contribute to its ability to support

*Address Correspondence to: Lawrence J. Bonassar, PhD., Professor, Department of Biomedical Engineering, 149 Weill Hall, Cornell University, Ithaca, NY 14853, (607) 255-9381, lb244@cornell.edu.
Mary Clare McCorry, M.S., Meinig School of Biomedical Engineering, 151 Weill Hall, Cornell University, Ithaca, NY 14853, mcm338@cornell.edu

Declaration of Interest

The authors report no conflicts of interest. The authors alone are responsible for the content and writing of the paper.

loads in the knee (1). The meniscus is connected to the underlying bone through a meniscal enthesis located at each of the meniscal horns (2,3). The meniscal entheses provide an anchor point for the meniscus to support tensile loads and prevent meniscal extrusion during the gait cycle (4). A majority of the fibers in the meniscus are arranged in the circumferential direction (5,6). A smaller portion of radial tie fibers help to anchor the circumferential fibers and contribute to the anisotropic properties of the meniscus (5,7,8). GAGs make up a smaller fraction of the meniscus and contribute its compressive properties (1,9,10).

Damage to the meniscus disrupts this organization, increasing contact pressure in the joint resulting in pain, swelling, and loss of motion (11,12). Since the meniscus is primarily avascular, surgical intervention is the primary treatment option. There are over 1 million meniscus related surgeries in the United States per year (13). In severe cases of injury or degeneration, a meniscal allograft is used to replace the damaged meniscus. While meniscal allografts relieve patient pain and restore mechanical stability to the knee, allograft transplant is limited by material availability, cost, immune competency, and ability to correctly match anatomic size and shape (14,15). Size matching must be within a tolerance of 5%, the donor must have less than mild pre-existing arthrosis, and be immunocompatible with recipient (14,15). Synthetic scaffold such as Menaflex and Actifit are used for partial meniscal replacement, however results are inconclusive as to their efficacy with specific challenges in tissue fixation, integration, material properties, and surface characteristics (16–18). An anatomically accurate tissue engineered (TE) meniscus could address many of these limitations by using imaging techniques to recapitulate size and shape, as well as natural materials, and autologous cells with the ability to modify and integrate with native tissue (19,20).

Previous efforts to TE the whole meniscus utilize synthetic polymers, hydrogels, and tissue-derived scaffolds (21–25). However, none of these are currently in clinical practice because they lack the anatomical, mechanical or biochemical properties necessary for native function (19). Previously, we developed an anatomically accurate tissue engineered meniscus using fibrochondrocytes (FCCs) in a high density collagen gel (26). FCCs, embedded in the meniscal construct, developed large fibers under static mechanical boundary conditions with mechanical properties approaching native values (27).

These studies show great promise, however, FCCs used for tissue engineered menisci have limited clinical availability and are difficult to expand in 2D culture (28). Obtaining the sufficient number of cells for a tissue engineered meniscus is challenging because FCCs proliferate slowly and often lose their phenotype in two-dimensional (2D) culture (28). Mesenchymal stem cells (MSCs) have been shown to contribute to meniscal regeneration *in vivo*, however, there is limited knowledge on MSC performance in the context of whole tissue engineered menisci (29–31). *In vivo* studies in both animals and humans have shown that MSCs delivered through intraarticular injection localize to the site of injury and contribute to tissue regeneration (30–33). However directing fibrochondrogenic differentiation of stem cells has proven to be challenging (34–36). Co-culture of FCCs and MSCs has been particularly successful with increased expression of fibrochondrogenic genes, reduced hypertrophy, and increased matrix production (35,36). We have shown that

MSCs transition to a fibrochondrogenic phenotype in 3D collagen gel, with maximal mechanical performance and GAG retention observed in the 50:50 co-culture group (37). Furthermore, MSCs have been shown to increase the lubrication properties of a engineered menisci (38). These studies suggest the potential advantages and feasibility of MSCs as an alternative or supplemental cell source for meniscus tissue engineering.

A successful tissue engineered meniscus must have organized fibers, which are essential to the mechanical stability of the meniscus in the knee (7). MSC differentiation is known to be guided by mechanical cues, specifically in meniscal development the meniscus begins as a dense mesenchymal condensate. In meniscus tissue engineering, MSCs have been shown to produce collagen and GAG that perform similar mechanical functions to native when seeded in an aligned matrix (39). The meniscus develops from a dense disorganized mesenchymal condensate (40). However, there is little data on MSCs produce a functionally organized fibers from a disorganized matrix. Anchoring at the attachments provides critical mechanical signals for collagen organization and matrix secretion (27,40,41). However there is little data on how mechanical anchoring affects MSCs in the context of producing a functionally organized meniscus.

The goal of this study was to characterize matrix synthesis and fiber formation in MSC and FCC co-culture in collagen gels. Specifically, we evaluated GAG accumulation and fiber formation in mono- and co-cultured menisci anchored at the horns. MSCs and FCCs differ in their ability to synthesize GAGs, however little is known about MSCs ability to form large organized fibers. We hypothesize that MSCs will have similar fiber organization and matrix producing capabilities as FCCs for the production of a tissue engineering meniscus.

Materials and Methods

Cell Isolation

As previously described, MSCs were isolated from 1–3 day old bovids (26,42). Briefly, the bone marrow from the trabeculae of the distal femoral head was washed with a heparin supplemented media to obtain the MSCs (37,42). Heparin solution containing bone marrow was centrifuged at 300 × *g*. The adherent cell population after 48 hours was expanded and tested to confirm multipotency using trilineage differentiation assays for osteogenesis, adipogenesis, and chondrogenesis (Supp. 1) (43,44). MSCs were plated at 2,000 cells/cm^2 and expanded in 2D culture until passage 4 with a growth medium containing low glucose Dulbecco's modified Eagle's medium (DMEM) supplemented with 10% fetal bovine serum (FBS), 100 μg/mL penicillin, 100 μg/mL streptomycin, 0.25 μg/mL amphotericin B, 2mM L-glutamine, and 1 ng/mL basic fibroblast growth factor.

FCCs were isolated from juvenile bovine menisci digested using collagenase as previously described (26,45). FCCs were digested from menisci in 0.3% collagenase (Worthington Biochemical Corporation, Lakewood, NJ) in DMEM with 100 μg/mL penicillin and 100 μg/mL streptomycin, followed by filtering through a 100 μm cell strainer (26,45). FCCs were directly encapsulated in collagen gels with passaged MSCs as described in construct generation. Prior to injecting cells into meniscal molds, MSCs were labeled using CellTrace Green CFSE (Invitrogen, Grand Island, NY, C34554) and FCCs were labeled with CellTrace

FarRed DDAO-SE (Invitrogen, C34553). Cell types were mixed with media to generate FCC mono-culture, 50/50 co-culture, and MSC mono-culture groups.

Construct Generation

Collagen type I was extracted from Sprague-Dawley rat tails (Pel-Freez Biologicals, Rogers, AZ) and reconstituted in 0.1% acetic acid at 30 mg/mL concentration as previously described (26,46,47). To initiate gelation, a syringe stop cock was used to mix the stock collagen solution with a working solution comprised of 1N NaOH, 10× phosphate-buffered saline (PBS), and 1× PBS to return the collagen to a neutral 7.0 pH and 300mOsm (47). Previously prepared cell groups suspended in media were mixed to a final concentration of 25×10^6 cells/mL in a collagen gel at 20 mg/mL (26). The collagen solution was injected into an anatomically accurate meniscal mold and incubated for 1 hour at 37˚C (27). Anatomically accurate molds were 3D printed from negative molds rendered using magnetic resonance imaging and microcomputed tomography images of ovine menisci (27,48). As described previously, injection molding into anatomically accurate meniscal molds yields a construct with high geometric fidelity to native tissue, within ±10% error of key geometric features (49,50). Anatomical molds included extension tabs at the horns for clamping (27,48).

Eight menisci per group, with four tested at day 1 and the remaining four tested after 4 weeks. Each meniscus was clamped at the extensions to a 3D printed culture dish as previously described (27). Clamping at the extensions mimics the static mechanical boundary conditions of the native meniscus. Samples were cultured in media containing DMEM, 10% FBS, 100 μg/mL penicillin, 100 μg/mL streptomycin, 0.1 mM non-essential amino acids, 50 μg/mL ascorbate, and 0.4 mM L-proline at 37°C and 5% CO_2 (26). Culture media was collected and replenished three times a week. Images were taken at each media change and imported into ImageJ to calculate the area of each construct. At the conclusion of culture, each meniscus was sectioned to obtain samples for biochemical, histological, and SEM analysis (Figure 1).

Biochemical Content

Biochemical samples were collected from four different regions on each meniscus. Each sample was weighed to obtain a wet weight (WW) then frozen, lyophilized, and weighed again to obtain dry weight (DW). As previously described, biochemical content of constructs was measured using a Hoechst DNA assay for DNA content (51), a modified 1,9-dimethylmethylene blue (DMMB) assay at pH 1.5 for GAG content (52) and a hydroxyproline (hypro) assay for collagen content (53). The same assays were performed on both constructs and media samples. The sum of biochemical content in media added to biochemical content in the construct was the total content. Retention was calculated as a percentage of content in each construct relative to total content.

Confocal Microscopy

At the conclusion of each culture period, menisci were sectioned with two slices taken from each meniscus, one each for radial and circumferential imaging (Figure 1). Samples were placed in 10% buffered formalin for 48 hours followed by storage in 70% ethanol. Confocal

reflectance, autofluorescence, and fluorescence imaging was performed on a Zeiss 710 confocal microscope with a Zeiss Axio Observer Z1 inverted stand using a 40×/1.2 C-Apochromat water immersion objective. Collagen fiber reflectance was captured between 475–510 nm, while cell autofluorescence was captured between 500–580 nm (26).

Images were analyzed for fiber diameter and alignment index (AI) by a custom MATLAB code as previously described (27,48,54). A circumferential cross-section was obtained from each meniscus in which 5-7 images from different regions of the cross-section were taken for analysis. Images were analyzed using a series of fast Fourier transforms (FFT) to determine alignment index followed by a radon transform to determine mean fiber diameter. A 2D FFT determines the maximum angle of alignment. An average cycle count along the x-axis perpendicular to the maximum angle of alignment was converted to pixels and then microns to determine the average diameter. The AI is a ratio of the number of fibers ±20° from the maximum angle of alignment divided by the predicted number of fibers in a 40° span (54). A sample with no alignment would have an AI of 1 and a sample with perfect alignment would have an AI of 4.5. Native menisci have an average AI of 1.8 in the circumferential direction.

Scanning Electron Microscopy

A 2-4 mm thick slice was obtained from each sample and prepared for scanning electron microscopy (SEM) (55). Samples were fixed overnight in 2.5% glutaraldehyde and then washed with a 0.05 M cacodylate buffer. Samples were then incubated with 2% osmium tetroxide for 1 hour as a secondary fixative. Following fixation, samples were dehydrated in a graded ethanol series over several days. Samples were dried using a critical point dryer and freeze fractured at the imaging face. Samples were coated with gold palladium prior to SEM imaging. Samples were imaged using a Tescan Mira3 FESEM.

Histology

Following confocal imaging, samples were dehydrated in a graded ethanol series, embedded into paraffin blocks, sectioned, and stained. For each sample, one section was embedded to examine the radial direction, with the second section embedded to examine the circumferential direction. Collagen was characterized using a picrosirious red staining, first imaged using brightfield microscopy and then visualized under polarized light to view collagen fiber organization (26). Immunohistochemistry (IHC) was conducted as previously described to further investigate collagen content using antibodies for collagen type I (Abcam, Cambridge, MA, 34710), collagen type II (Chondrex, Redmond, WA, 7005), and collagen type X (Abcam, 58632) (37). Specific proteoglycans including biglycan (courtesy of Dr. Larry Fischer, NIDCR, LF-96), decorin (courtesy of Dr. Larry Fischer, NIDCR, LF-94), and fibromodulin (Abcam, 81443). Primary and secondary antibody controls were run in parallel with samples for immunohistochemistry stains (Supplemental 1 and 6). All slide were counterstained with hematoxylin. Images were obtained with a SPOT RT camera (Diagnostic Instruments, Sterling Heights, MI) attached to a Nikon Eclipse TE2000-S microscope (Nikon Instruments, Melville, NY).

Enzyme-Linked Immunosorbent Assay (ELISA)

Small tissue specimens were obtained from each samples and assayed for collagen type I and II using ELISA. Tissue was lyophilized, pulverized, and weighed for dry weight. ~2 mg of tissue was extracted using a series of 4°C incubations with guanidine, acetic acid, pepsin and elastase. Prior to assaying, the level of solubilization was evaluated via a 6% SDS-gel stained using Coomassie Blue with collagen II as a standard. A three day solubilization period with pepsin was used to digest tissue. Levels of collagen was detected using a bovine type I and multispecies type II collagen detection kits (Chondrex, Redmond, WA).

Mechanical Properties

Two 4 mm diameter plugs from each sample were tested for compressive properties (49,56,57). Each sample was tested in confined compression via a stress relaxation test performed by imposing 10×100 μm steps (relaxation=12 min., strain=5-45%, steps=5%, n=4). The measured loads were fit to a poroelastic model using a custom MATLAB program to determine aggregate modulus (HA). A dog bone punch in the radial and circumferential direction was obtained from each samples and tensile tested (Figure 1). A 0.75%/sec strain rate was applied to mimic quasistatic loading and the elastic modulus was measured as the slope of the linear region of the stress vs strain curve. Mechanical testing was performed on an Enduratec ElectroForce 3200 System (Bose, Eden Prairie, MN) using a 250 g or 1 kg load cell.

Statistics

Contraction data was analyzed using a 2-way-ANOVA with Tukey's t-test for post hoc analysis. Biochemical and ELISA data were analyzed by 1-way-ANOVA using Tukey's t-test for post hoc analysis. A mixed model with random effect of sample number was used for fiber diameter and fiber alignment data. Fiber diameter had an inter class correlation coefficient (ICC) of 13% and fiber alignment had an ICC of 4%. Biochemical content was compared to fiber formation measures using a least square fit and significance was determined using a Pearson correlation. All data are written as mean ±SD and significance was determined with $p<0.05$. Data analysis was conducted using JMP software (SAS Institute Inc, Cary, NC).

Results

Cell type does not influence contraction

Throughout culture, constructs maintained anatomical size and shape. Constructs had minimal contraction, contracting uniformly to maintain shape with a loss of ~25% projected area (Figure 2). All three culture groups contracted gradually over time with no significant differences in contraction between groups at each time point ($p>0.05$) (Figure 2A). Constructs maintained anatomical definition throughout the 4 weeks of culture (Figure 2B).

MSC, 50/50, and FCC culture groups organized oriented fibers

At the beginning of culture, menisci had small disorganized fibers (~8.5 μm in diameter and 1.35 AI) with a homogenous cell distribution (Figure 4). After 4 weeks in culture, fibers

become more organized with regions of directionally oriented fibers. Fiber alignment was directionally dependent, circumferential and radial faces were imaged from different locations from each sample (Figure 3). In the circumferential direction collagen fibers were oriented in the circumferential direction running from horn to horn where each sample was clamped at an extension. FCC mono-culture menisci had visible striations analogous to fiber fascicles seen in native meniscal fibers (Figure 3). A thin, aligned outer edge with radial fibers extending into the bulk of the tissue was apparent in radially sliced samples. MSC mono-culture group showed early signs of fiber development and alignment, however, fibers appeared smaller than those in FCC mono-culture and 50/50 co-culture groups.

FCC mono-culture have the greatest fiber diameter

Image analysis of circumferential images quantified the fiber diameter and alignment index in samples groups. Consistent with qualitative image observations, FCC mono-cultured menisci produced significantly larger diameter fibers and more aligned fibers than 50/50 and MSC cultured menisci ($p<0.05$). FCC mono-culture had the highest fiber diameter at ~17 μm and MSC mono-culture had the lowest fiber diameter at ~9 μm (Figure 4). The 50/50 co-culture had a diameter in between FCC and MSC mono-culture at ~12 μm. After 4 weeks in culture FCC fiber diameter approached native values averaging at ~35 μm. A similar trend was observed in the alignment index, where FCCs had increased fiber diameter and alignment approaching native values at ~1.75 (27,48).

MSCs transition to chondrogenic morphology while FCCs integrate into collagen fibers

FCCs and MSCs labeled with cell tracker dyes were imaged at the beginning of culture and after 4 weeks of culture. FCCs and MSCs were evenly distributed throughout the depth of the meniscus construct. The FCCs and MSCs in the 50/50 co-culture group were homogenously mixed and distributed throughout the gel at the beginning of culture (Figure 5 row 1). At 0 weeks FCCs appeared small and rounded, while MSCs were slightly larger in size and appeared elongated on the collagen gel (Figure 5 row 2). After 4 weeks of culture in a fibrochondrogenic media, cells remained evenly distributed throughout the collagen. While the FCCs remained in a circular phenotype, MSCs transitioned from an elongated morphology consistent with a fibroblastic phenotype to a circular morphology consistent with a chondrogenic morphology (Figure 5 row 3). Collagen gels have small disorganized fibers at 0 weeks that develop into larger more organized fibers after 4 weeks. The FCC mono-culture group formed well defined fibers where FCCs integrated into the collagen fibers. The MSC mono-culture group had less developed fibers and MSCs settled into pores between collagen fibers (Figure 5 row 4).

MSCs increased matrix production compared to FCCs

The presence of MSCs in tissue engineered meniscal constructs increased GAG and collagen accumulation. After 4 weeks in culture, the MSC mono-culture menisci had ~350% more GAG/meniscus and the 50/50 co-culture had ~250% more GAG/meniscus than the FCC mono-culture group (Figure 6A). Similar trends were noted when GAG content was normalized to DNA (Figure 6B). GAG content measured in the media was added to GAG content in the menisci to calculate retention of GAG in the constructs relative to total GAG produced. 50/50 co-culture retained a significantly higher amount of GAG in each meniscus

sample (Figure 6C). 50/50 co-culture and MSC mono-culture showed an increase in production of hydroxyproline compared to FCC mono-culture, however this increase was not significant (Figure 6D, $p>0.05$). Tissue engineered menisci when seeded with MSCs have ~30 % of the GAG (μg)/ww(mg) and 40% hypro(μg)/ww(mg) content of human native menisci, while tissue engineered constructs seeded with FCCs have ~12% and 31% respectively (wet weights presented in Supplemental Figure 2)(58). Seeding constructs with MSCs improved the biochemical content to better resemble native values.

Collagen and proteoglycans were probed in meniscus scaffolds using immunohistochemistry and ELISA (Figure 8 and Supplemental 5). MSC mono-cultured constructs had increased levels of staining for biglycan and decorin with heavy staining at the surface of the construct. FCC mono-cultured constructs had increased staining of fibromodulin throughout the depth of the construct (Supplemental 5). Meniscus scaffolds were initially cast using collagen type I. Positive staining for collagen type I was consistent between 0 and 4 weeks. After 4 weeks in culture FCC mono-culture stained darker for collagen type II compared to the other culture groups. ELISA analysis supports that FCC and 50/50 groups produce more collagen type II than MSC seeded menisci. Conversely, MSC seeded menisci produced significantly more collagen type I than FCC and 50/50 groups (Supplemental 3). Minimal staining for collagen type X was seen in culture groups.

Fiber diameter was inversely correlated with GAG content

While MSCs have an increased ability to generate GAG and hydroxyproline, constructs seeded with MSCs have smaller collagen fibers. Fiber diameter and alignment index were compared with GAG and hydroxyproline content per construct using a linear regression and Pearson correlation (Figure 7). Hydroxyproline content was not correlated with fiber diameter and alignment index. Alignment index had a statistical tend of decreasing as GAG content increased ($R^2=0.38$, $p<0.056$). Fiber diameter and GAG content per meniscus were negatively correlated with fiber diameter decreasing with increasing GAG content ($R^2=0.85$, $p<0.05$).

Mechanical properties improve with time in culture

Meniscal constructs increased in both tensile and compressive modulus after 4 weeks in culture (Supplemental 4). Samples from the circumferential and radial direction were not statistically different and were therefore pooled. Tensile properties were highest in the MSC group (60 kPa) and compressive properties were highest in the FCC group (59 kPa). Tissue engineered menisci are at about 15% of native bovine aggregate modulus, however tensile value are still far below native values (59,60). While construct properties increased with time, there was no significant difference between culture groups after 4 weeks.

Discussion

The objective of this study was to evaluate GAG production and fiber formation of MSCs in mono- and co-culture with FCCs. This study showed that MSCs incorporated in a 3D tissue engineered meniscus had increased matrix production, but decreased the fiber reorganization compared to FCCs. This study demonstrated that while MSCs in this system are highly

metabolically active, producing collagen and GAG, the types of collagen and the organization of the collagen network are different between MSCs and FCCs.

Maintenance of size and shape is a critical factor in engineering anatomical meniscus implants. We have previously shown that anchoring a FCC seeded implant at the horns reduced collagen contraction (27). MSCs are known to be a highly proliferative and contractile cell type (44,61–65). The proliferative properties of stem cells are desirable for obtaining sufficient cell numbers for construct generation, however precise control over contraction is important for matching the size and shape of tissue engineered menisci for clinical application. MSCs are known to rapidly contract low density collagen matrixes along a mechanically fixed axis (61,63,64). High concentration collagen with a mechanical boundary condition is known to reduce collagen contraction (26,27,47,66). Given MSCs highly contractile nature, monitoring of anatomical size and shape throughout culture is important for determining if MSCs are an appropriate cell type for use in meniscus tissue engineering. In this study, MSCs were embedded in tissue engineered menisci both in co-culture with FCC and in mono-culture. Changing the cell type had no significant influence on meniscal contraction. This study shows that the use of MSCs in tissue engineered meniscus has minimal impact on the overall size and shape of the meniscus.

In addition to maintaining anatomical shape, a key challenge in meniscus tissue engineering is generating appropriate microstructure and fiber organization. Mechanical constraints are a well-established method used to direct cellular remodeling and guide the alignment of fibers in collagen gels. This has been shown across many systems and cell types including collagen seeded with MSCs (61,64,65), fibroblasts (41,67–69), and annulus fibrosis chondrocytes (46). The mechanical fixation used in this study mimics native fixation at the meniscal enthesis (70). Application of a mechanical constraint at the meniscal horns has been shown to create native like orientation of fibers in a tissue engineered meniscus seeded with FCCs (27). However, there is limited research on MSCs ability to form fibers in the context of meniscus. In other systems for tendon and ligament tissue engineering, MSCs are able to exert tractional forces and align fibers in the direction of axial fixation (61,62,65,67). Contraction was often coupled with fiber formation, however contraction and fiber formation are dependent on the mechanical load, collagen concentration, and cell concentration (61,63,64). Furthermore, contraction does not directly correlate to fiber formation. Previously we have seen that groups with increased contraction had decreased fiber size and alignment, where mechanical fixation had a greater effect on fiber formation (27). Another study saw found that MSCs seeded on an aligned matrix had limited GAG and collagen production compared to FCCs seed on the same matrix (71). In the study, MSCs developed and formed fibers, however MSC fiber diameter and alignment were inferior to FCCs. Native fiber diameters are ~35 μm and with an alignment index of ~1.75 (27,48). Of the three culture groups, the FCC mono-culture menisci were closest to native values at a diameter of ~17 μm and an alignment index of ~1.47. Both FCC mono-culture and co-culture have significant increases in fiber diameter, however, MSC mono-cultured menisci do not significantly increase fiber diameter after 4 weeks of culture. These findings emphasize that FCCs and MSCs have different responses to the mechanical boundary conditions and the structural microenvironment they are cultured in.

Proteoglycans are another factor known to influence the nature of fiber formation. The data from this study showed that increasing GAG content was inversely correlated with decreasing fiber diameter. Notably, the production of GAG was significantly higher in the MSC mono-cultured gels which had the lowest fiber diameter. In this study, MSC mono-cultured gels had ~350% and co-cultured gels had ~250% the amount of GAG/meniscus compared to FCC mono-culture. While GAG production is typically considered a positive marker for a meniscal phenotype, the concentration of GAG in the meniscus is significantly lower than cartilage, with proteoglycans only comprising 1-2% of the dry weight (1,72,73). Furthermore the GAG content of the meniscus increases with age until skeletal maturity (72). The type of GAG can influence the way in which fibers form. Small leucine rich proteoglycans (SLRPs) are present in fibrocartilage and play a key role in matrix assembly (10,74,75). The presence of certain small proteoglycans may actually lead to decreased fiber forming capabilities by inhibiting assembly of collagen fibrils (76–78). The constructs in this study produced SLRPs decorin, biglycan, and fibromodulin. The increased production of GAG in the MSC cultures was correlated with the reduced ability to form large fibers. Over accumulation of SLRPs has been linked with reduced fibrillogenesis, however more research into the interaction and concentration of these molecules in the meniscus is necessary to better understand how to influence fiber formation for tissue engineering (78,79). While MSCs are the native cell precursor to FCCs in development this system does not adequately differentiate MSCs into FCCs with the same fiber forming capabilities. Fine tuning the amount and types of proteoglycans produced by FCCs and MSCs will provide insight into their role in controlling fiber formation.

The meniscus is known to be largely comprised of water, collagen, and proteoglycans (10,80). Collagen type I is highly prevalent in the outer red-red zone and collagen type II is the predominant collagen type in the inner white-white zone (81). Tissue engineered menisci in this study contained both collagen I and collagen II. MSC seeded constructs produced significantly higher amounts of collagen type I, whereas FCC and co-cultured constructs showed increased levels of collagen type II. At 4 weeks, there were no spatial differences in the expression between collagen type I and II. Collagen type I is found in a region of the meniscus typically under tensile stresses, while collagen type II is prevalent in the inner meniscus typically under more compressive loads (20). The menisci in this study are constrained at the horns providing a static mechanical boundary condition. A dynamic loading regime mimicking native mechanical loading would likely increase regional expression of collagen types resembling native meniscus (48).

The specific use of MSCs in a tissue engineered model of meniscus formation could lend key insight into the development of native meniscus. During the development of the knee, the meniscus begins as a dense mesenchymal condensate (40,82). Throughout embryonic development cellular concentration decreases as collagen content increases (40,83) Collagen fibers begin as small and disorganized and gradually begin to form larger organized fibers after establishment of the meniscal insertions. Early fiber alignment is established in embryonic development, however meniscal maturity is not reached until after years of normal load bearing in a child (40,84). GAG content is low in early development when fibers form, with age, GAGs are deposited in distinct domains separate from collagen (72,74,85) Mechanical load bearing is essential to the maturation of the meniscus both pre-

and post-natally (86). Similar to early stages of meniscal development, our system begins culture with MSCs seeded into a disorganized collagen gel. Similar to enthesis fixation during development, mechanical fixation at the horns helps to direct fiber formation. Tissue engineered menisci seeded with MSCs mimic the developmental process which will help to inform chemical and mechanical signals that may play a role in meniscal development. The system established in this study can be used to ask specific questions about how mechanical and biochemical signals can influence MSC differentiation and meniscal development.

This study compared the ability of MSCs and FCCs to form a large organized meniscal implant. MSCs produced an anatomically accurate TE meniscus with high levels of GAG, however the tissue had inferior fiber microstructure. High levels of GAG are typically considered positive markers for fibrochondrogenic differentiation, however this study indicates that high levels of GAG production is correlated with reduced fiber diameter. MSCs remain a promising cell source for tissue engineering, however achieving targets for fiber size and organization will likely require manipulating the amount and types of GAGs produced by MSCs. In this study, co-cultures achieved intermediate levels fiber formation and GAG production. Co-culture can be used as a technique to utilize the fiber formation capabilities of FCC and the matrix production properties of MSCs while reducing the clinical dependence on high volumes of FCCs for tissue engineering the meniscus.

Supplementary Material

Refer to Web version on PubMed Central for supplementary material.

Acknowledgments

The authors would like to thank Dr. Jennifer L. Puetzer. This work made use of the Cornell Center for Materials Research Shared Facilities which are supported through the NSF MRSEC program (DMR-1120296) and Cornell University Biotechnology Resource Center (BRC) which is supported through NIH S10RR025502, NYSTEM CO29155 and NIH S10OD018516.

Funding

This investigation was supported by National Center for Advancing Translational Sciences (NCATS) grant TL1TR000459 of the Clinical and Translational Science Center at Weill Cornell Medical College.

References

1. McDevitt CA, Webber RJ. The ultrastructure and biochemistry of meniscal cartilage. Clin Orthop Relat Res. 1990; 252:8–18.
2. Kohn D, Moreno B. Meniscus insertion anatomy as a basis for meniscus replacement: a morphological cadaveric study. Arthroscopy. 1995; 11(1):96–103. [PubMed: 7727019]
3. Messner K, Gao J. The menisci of the knee joint. Anatomical and functional characteristics, and a rationale for clinical treatment. J Anat. 1998; 193(Pt 2):161–78. [PubMed: 9827632]
4. Pagnani MJ, Cooper DE, Warren RF. Extrusion of the medial meniscus. Arthrosc J Arthrosc Relat Surg. 1991; 7(3):297–300.
5. Petersen W, Tillmann B. Collagenous fibril texture of the human knee joint menisci. Anat Embryol (Berl). 1998; 197(4):317–24. [PubMed: 9565324]
6. Kambic HE, McDevitt CA. Spatial organization of types I and II collagen in the canine meniscus. J Orthop Res. 2005; 23(1):142–9. [PubMed: 15607886]

7. Skaggs DL, Warden WH, Mow VC. Radial tie fibers influence the tensile properties of the bovine medial meniscus. J Orthop Res. 1994; 12(2):176–85. [PubMed: 8164089]
8. Andrews SHJ, Rattner JB, Abusara Z, Adesida A, Shrive NG, Ronsky JL. Tie-fibre structure and organization in the knee menisci. J Anat. 2014 May; 224(5):531–7. [PubMed: 24617800]
9. Melrose J, Smith S, Cake M, Read R, Whitelock J. Comparative spatial and temporal localisation of perlecan, aggrecan and type I, II and IV collagen in the ovine meniscus: An ageing study. Histochem Cell Biol. 2005; 124(3–4):225–35. [PubMed: 16028067]
10. Nakano T, Dodd CM, Scott PG. Glycosaminoglycans and proteoglycans from different zones of the porcine knee meniscus. J Orthop Res. 1997; 15(2):213–20. [PubMed: 9167623]
11. Greis PE, Bardana DD, Holmstrom MC, Burks RT. Meniscal injury: I. Basic science and evaluation. J Am Acad Orthop Surg. 2002; 10(3):168–76. [PubMed: 12041938]
12. Bedi A, Kelly NH, Baad M, Fox AJS, Brophy RH, Warren RF, et al. Dynamic contact mechanics of the medial meniscus as a function of radial tear, repair, and partial meniscectomy. J Bone Joint Surg Am. 2010; 92(6):1398–408. [PubMed: 20516315]
13. Khetia EA, McKeon BP. Meniscal allografts: biomechanics and techniques. Sports Med Arthrosc. 2007 Sep; 15(3):114–20. [PubMed: 17700370]
14. Brophy RH, Matava MJ. Surgical Options for Meniscal Replacement. J Am Acad Orthop Surg. 2012; 20(5):265–72. [PubMed: 22553098]
15. Verdonk, R., Volpi, P., Verdonk, P., Van Der Bracht, H., Van Laer, M., Almqvist, KF., et al. Indications and limits of meniscal allografts Injury. Vol. 44. Elsevier Ltd; 2013. p. S21-7.
16. Food and Drug Administration. Review of the ReGen Menaflex: Departures from Processes, Procedures, and Practices Leave the basis for a REview Decision in Question [Internet]. 2009 Available from: Food and Drug.
17. Maher, Sa, Rodeo, Sa, Doty, SB., Brophy, R., Potter, H., Foo, L-F., et al. Arthroscopy. Vol. 26. Elsevier Inc; 2010 Nov. Evaluation of a porous polyurethane scaffold in a partial meniscal defect ovine model; p. 1510-9.
18. Fox AJS, Wanivenhaus F, Burge AJ, Warren RF, Rodeo Sa. The human meniscus: A review of anatomy, function, injury, and advances in treatment. Clin Anat. 2015; 28(2):269–87. [PubMed: 25125315]
19. Makris, E., Hadidi, P., Athanasiou, K. Biomaterials. Vol. 32. Elsevier Ltd; 2011 Oct. The knee meniscus: structure-function, pathophysiology, current repair techniques, and prospects for regeneration; p. 7411-31.
20. Sweigart, Ma, Athanasiou, Ka. Toward tissue engineering of the knee meniscus. Tissue Eng. 2001 Apr; 7(2):111–29. [PubMed: 11304448]
21. Mandal, BB., Park, S-H., Gil, ES., Kaplan, DL. Biomaterials. Vol. 32. Elsevier Ltd; 2011 Jan. Multilayered silk scaffolds for meniscus tissue engineering; p. 639-51.
22. Messner K. Meniscal substitution with a Teflon-periosteal composite graft: a rabbit experiment. Biomaterials. 1994 Mar; 15(3):223–30. [PubMed: 8199295]
23. Wood DJ, Minns RJ, Strover A. Replacement of the rabbit medial meniscus with a polyester-carbon fibre bioprosthesis. Biomaterials. 1990 Jan; 11(1):13–6.
24. Stabile, KJ., Odom, D., Smith, TL., Northam, C., Whitlock, PW., Smith, BP., et al. Arthrosc J Arthrosc Relat Surg. Vol. 26. Elsevier Inc; 2010 Jul. An acellular, allograft-derived meniscus scaffold in an ovine model; p. 936-48.
25. de Groot JH, Zijlstra FM, Kuipers HW, Pennings AJ, Klompmaker J, Veth RPH, et al. Meniscal tissue regeneration in porous 50/50 copoly (L-lactideh-caprolactone) implants. 1997; 18(8):613–22.
26. Puetzer, JL., Bonassar, LJ. Acta Biomater. Vol. 9. Acta Materialia Inc; 2013 May 10. High Density Type I Collagen Gels for Tissue Engineering of Whole Menisci; p. 7787-95.
27. Puetzer JL, Koo E, Bonassar LJ. Induction of fiber alignment and mechanical anisotropy in tissue engineered menisci with mechanical anchoring. J Biomech Elsevier. 2015; 48(8):1436–43.
28. Gunja NJ, Athanasiou KA. Passage and reversal effects on gene expression of bovine meniscal fibrochondrocytes. Arthritis Res Ther. 2007 Jan.9(5):R93. [PubMed: 17854486]

29. Pittenger MF, Mackay AM, Beck SC, Jaiswal RK, Douglas R, Msca JD, et al. Multilineage Potential of Adult Human Mesenchymal Stem Cells. Science (80-). 1999 Apr 2; 284(5411):143–7.
30. Centeno, CJ., Busse, D., Kisiday, J., Keohan, C., Freeman, M., Karli, D. Med Hypotheses. Vol. 71. Elsevier Ltd; 2008 Dec. Regeneration of meniscus cartilage in a knee treated with percutaneously implanted autologous mesenchymal stem cells; p. 900-8.
31. Duygulu F, Demirel M, Atalan G, Kaymaz FF, Kocabey Y, Dulgeroglu TC, et al. Effects of intra-articular administration of autologous bone marrow aspirate on healing of full-thickness meniscal tear: an experimental study on sheep. Acta Orthop Traumatol Turc. 2012; 46(1):61–7. [PubMed: 22441454]
32. Agung M, Ochi M, Yanada S, Adachi N, Izuta Y, Yamasaki T, et al. Mobilization of bone marrow-derived mesenchymal stem cells into the injured tissues after intraarticular injection and their contribution to tissue regeneration. Knee surgery, Sport Traumatol Arthrosc Off J ESSKA. 2006 Dec; 14(12):1307–14.
33. Kim J-D, Lee GW, Jung GH, Kim CK, Kim T, Park JH, et al. Clinical outcome of autologous bone marrow aspirates concentrate (BMAC) injection in degenerative arthritis of the knee. Eur J Orthop Surg Traumatol. 2014 Jan.24:8. 1505–11.
34. Hoben GM, Willard VP, Athanasiou KA. Fibrochondrogenesis of hESCs: growth factor combinations and cocultures. Stem Cells Dev. 2009 Mar; 18(2):283–92. [PubMed: 18454697]
35. Saliken, DJ., Mulet-Sierra, A., Jomha, NM., Adesida, AB. Arthritis Res Ther. Vol. 14. BioMed Central Ltd; 2012 Jan. Decreased hypertrophic differentiation accompanies enhanced matrix formation in co-cultures of outer meniscus cells with bone marrow mesenchymal stromal cells; p. R153
36. Cui X, Hasegawa A, Lotz M, D'Lima D. Structured three-dimensional co-culture of mesenchymal stem cells with meniscus cells promotes meniscal phenotype without hypertrophy. Biotechnol Bioeng. 2012 Sep; 109(9):2369–80. [PubMed: 22422555]
37. McCorry MC, Puetzer JL, Bonassar LJ. Characterization of mesenchymal stem cells and fibrochondrocytes in three-dimensional co-culture: analysis of cell shape, matrix production, and mechanical performance. Stem Cell Res Ther Stem Cell Research & Therapy. 2016; 7(1):39.
38. Bonnevie, ED., McCorry, MC., Bonassar, LJ. Biotribology. Elsevier B.V; 2016. Mesenchymal Stem Cells Enhance Lubrication of Engineered Meniscus Through Lubricin Localization in Collagen Gels.
39. Nerurkar NL, Han W, Mauck RL, Elliott DM. Homologous structure-function relationships between native fibrocartilage and tissue engineered from MSC-seeded nanofibrous scaffolds. Biomaterials Elsevier Ltd. 2011; 32(2):461–8.
40. Clark CR, Ogden JA. Prenatal and Postnatal Development of Human Knee Joint Mensci. Iowa Orthop J. 1981; 1(1):20–7.
41. Costa KD, Lee EJ, Holmes JW. Creating alignment and anisotropy in engineered heart tissue: role of boundary conditions in a model three-dimensional culture system. Tissue Eng. 2003 Aug; 9(4): 567–77. [PubMed: 13678436]
42. Mauck RL, Yuan X, Tuan RS. Chondrogenic differentiation and functional maturation of bovine mesenchymal stem cells in long-term agarose culture. Osteoarthr Cartil. 2006 Feb; 14(2):179–89. [PubMed: 16257243]
43. Bernacki SH, Wall ME, Loboa EG. Isolation of human mesenchymal stem cells from bone and adipose tissue. Methods Cell Biol. 2008 Jan; 86(8):257–78. [PubMed: 18442651]
44. Mackay AM, Beck SC, Murphy JM, Barry FP, Chichester CO, Pittenger MF. Chondrogenic differentiation of cultured human mesenchymal stem cells from marrow. Tissue Eng. 1998 Jan; 4(4):415–28. [PubMed: 9916173]
45. Ballyns, JJ., Wright, TM., Bonassar, LJ. Biomaterials. Vol. 31. Elsevier Ltd; 2010 Sep. Effect of media mixing on ECM assembly and mechanical properties of anatomically-shaped tissue engineered meniscus; p. 6756-63.
46. Bowles RD, Williams RM, Zipfel WR, Bonassar LJ. Self-Assembly of Aligned Tissue-Engineered Annulus fibrosus and Intervertebral Disc Composite Via Collagen Gel Contraction. Tissue Eng Part A. 2010; 16(4)

47. Cross, VL., Zheng, Y., Won Choi, N., Verbridge, SS., Sutermaster, Ba, Bonassar, LJ., et al. Biomaterials. Vol. 31. Elsevier Ltd; 2010. Dense type I collagen matrices that support cellular remodeling and microfabrication for studies of tumor angiogenesis and vasculogenesis in vitro; p. 8596-607.
48. Puetzer JL, Bonassar LJ. Physiologically Distributed Loading Patterns Drive the Formation of Zonally Organized Collagen Structures in Tissue Engineered Meniscus. Tissue Eng Part A. 2016; (607):1–40.
49. Ballyns JJ, Gleghorn JP, Niebrzydowski V, Rawlinson JJ, Potter HG, Maher SA, et al. Image-guided tissue engineering of anatomically shaped implants via MRI and micro-CT using injection molding. Tissue Eng Part A. 2008 Jul; 14(7):1195–202. [PubMed: 18593357]
50. Ballyns JJ, Cohen DL, Malone E, Maher Sa, Potter HG, Wright T, et al. An optical method for evaluation of geometric fidelity for anatomically shaped tissue-engineered constructs. Tissue Eng Part C Methods. 2010 Aug; 16(4):693–703. [PubMed: 19788346]
51. Kim YJ, Sah RL, Doong JY, Grodzinsky AJ. Fluorometric assay of DNA in cartilage explants using Hoechst 33258. Anal Biochem. 1988; 174(1):168–76. [PubMed: 2464289]
52. Enobakhare BO, Bader DL, Lee DA. Quantification of sulfated glycosaminoglycans in chondrocyte/alginate cultures, by use of 1,9-dimethylmethylene blue. Anal Biochem. 1996; 243(1):189–91. [PubMed: 8954546]
53. Neuman R, Logan M. The determination of hydroxyproline. J Biol Chem. 1949; 184(1):299–306.
54. Bowles RD, Williams RM, Zipfel WR, Bonassar LJ. Self-assembly of aligned tissue-engineered annulus fibrosus and intervertebral disc composite via collagen gel contraction. Tissue Eng Part A. 2010; 16(4):1339–48. [PubMed: 19905878]
55. Moran JM, Pazzano D, Bonassar LJ. Characterization of polylactic acid-polyglycolic acid composites for cartilage tissue engineering. Tissue Eng. 2003; 9(1):63–70. [PubMed: 12625955]
56. Frank EH, Grodzinsky AJ. Cartilage electromechanics–II. A continuum model of cartilage electrokinetics and correlation with experiments. J Biomech. 1987; 20(6):629–39. [PubMed: 3611138]
57. Kim YJ, Bonassar LJ, Grodzinsky AJ. The role of cartilage streaming potential, fluid flow and pressure in the stimulation of chondrocyte biosynthesis during dynamic compression. J Biomech. 1995; 28(9):1055–66. [PubMed: 7559675]
58. Ala-Myllymäki J, Honkanen JTJ, Töyräs J, Afara IO. Optical spectroscopic determination of human meniscus composition. J Orthop Res. 2016; 34(2):270–8. [PubMed: 26267333]
59. Proctor CS, Schmidt MB, Whipple RR, Kelly Ma, Mow VC. Material properties of the normal medial bovine meniscus. J Orthop Res. 1989; 7(6):771–82. [PubMed: 2677284]
60. Peloquin JM, Santare MH, Elliott DM. Advances in quantification of meniscus tensile mechanics including nonlinearity, yield, and failure. J Biomech Eng. 2016; 138(2):021002. (13 pages). [PubMed: 26720401]
61. Awad HA, Butler DL, Harris MT, Ibrahim RE, Wu Y, Young RG, et al. In vitro characterization of mesenchymal stem cell-seeded collagen scaffolds for tendon repair: Effects of initial seeding density on contraction kinetics. J Biomed Mater Res. 2000; 51(2):233–40. [PubMed: 10825223]
62. Cai D, Marty-Roix R, Hsu H, Spector M. Lapine and Canine Bone Marrow Stromal cElls Contain Smooth Muscle Actin and Contract a Collagen-Glycosaminoglycan Matrix. Tissue Eng Part A. 2001; 7(6):829–41.
63. Juncosa-Melvin N, Boivin GP, Galloway MT, Gooch C, West JR, Sklenka AM, et al. Effects of cell-to-collagen ratio in mesenchymal stem cell-seeded implants on tendon repair biomechanics and histology. Tissue Eng. 2005; 11(3–4):448–57. [PubMed: 15869423]
64. Nirmalanandhan VS, Levy MS, Huth AJ, Butler DL. Effects of cell seeding density and collagen concentration on contraction kinetics of mesenchymal stem cell-seeded collagen constructs. Tissue Eng. 2006; 12(7):1865–72. [PubMed: 16889516]
65. Young RG, Butler DL, Weber W, Caplan a I, Gordon SL, Fink DJ. Use of mesenchymal stem cells in a collagen matrix for Achilles tendon repair. J Orthop Res. 1998; 16(4):406–13. [PubMed: 9747780]

66. Bell E, Ivarsson B, Merrill C. Production of a tissue-like structure by contraction of collagen lattices by human fibroblasts of different proliferative potential in vitro. Proc Natl Acad Sci U S A. 1979; 76(3):1274–8. [PubMed: 286310]

67. Huang D, Chang TR, Aggarwal A, Lee RC, Ehrlich HP. Mechanisms and dynamics of mechanical strengthening in ligament-equivalent fibroblast-populated collagen matrices. Ann Biomed Eng. 1993; 21(3):289–305. [PubMed: 8328728]

68. Thomopoulos S, Fomovsky GM, Holmes JW. The development of structural and mechanical anisotropy in fibroblast populated collagen gels. J Biomech Eng. 2005; 127(5):742–50. [PubMed: 16248303]

69. Grinnell F. Fibroblast-collagen-matrix contraction: growth-factor signalling and mechanical loading. Trends Cell Biol. 2000; 10(9):362–5. [PubMed: 10932093]

70. Abraham, AC., Haut Donahue, TL. Acta Biomater. Vol. 9. Acta Materialia Inc; 2013. From meniscus to bone: A quantitative evaluation of structure and function of the human meniscal attachments; p. 6322-9.

71. Baker BM, Nathan AS, Gee AO, Mauck RL. The influence of an aligned nanofibrous topography on human mesenchymal stem cell fibrochondrogenesis. Biomaterials. 2010; 31(24):6190–200. [PubMed: 20494438]

72. McNicol D, Roughley PJ. Extraction and characterization of proteoglycan from human meniscus. Biochem J. 1980; 185(3):705–13. [PubMed: 6892987]

73. Kawamura S, Lotito K, Rodeo SA. BIOMECHANICS AND HEALING RESPONSE OF. 2003; 11(2):68–76.

74. Vanderploeg EJ, Wilson CG, Imler SM, Ling CHY, Levenston ME. Regional variations in the distribution and colocalization of extracellular matrix proteins in the juvenile bovine meniscus. J Anat. 2012; 221(2):174–86. [PubMed: 22703476]

75. Hayes AJ, Isaacs MD, Hughes C, Caterson B, Ralphs JR. Collagen fibrillogenesis in the development of the annulus fibrosus of the intervertebral disc. Eur Cells Mater. 2011; 22(0):226–41.

76. Vogel KG, Paulsson M, Heinegård D. Specific inhibition of type I and type II collagen fibrillogenesis by the small proteoglycan of tendon. Biochem J. 1984; 223(3):587–97. [PubMed: 6439184]

77. Vogel KG, Trotter JA. The Effect of Proteoglycans on the Morphology of Collagen Fibrils Formed In Vitro. Coll Relat Res Gustav Fischer Verlag · Stuttgart · New York. 1987; 7(2):105–14.

78. Viola M, Bartolini B, Sonaggere M, Giudici C, Tenni R, Tira ME. Fibromodulin interactions with type I and II collagens. Connect Tissue Res. 2007; 48(3):141–8. [PubMed: 17522997]

79. Wang VM, Bell RM, Thakore R, Eyre DR, Galante JO, Li J, et al. Murine tendon function is adversely affected by aggrecan accumulation due to the knockout of ADAMTS5. J Orthop Res. 2012; 30(4):620–6. [PubMed: 21928430]

80. Eyre DR, Koob TJ, Chun LE. Biochemistry of the meniscus: unique profile of collagen types and site-dependent variations in composition. Orthop Trans. 1983; 8(53)

81. Cheung HS. Distribution of type I, II, III and V in the pepsin solubilized collagens in bovine menisci. Connect Tissue Res. 1987; 16(4):343–56. [PubMed: 3132349]

82. Gray DJ, Gardner E. Prenatal development of the human knee and superior tibiofibular joints. Am J Anat. 1950; 86(2):235–87. [PubMed: 15410671]

83. Mérida-Velasco, Ja, Sánchez-Montesinos, I., Espín-Ferra, J., Rodríguez-Vázquez, JF., Mérida-Velasco, JR., Jiménez-Collado, J. Development of the human knee joint. Anat Rec. 1997 Jun; 248(2):269–78. [PubMed: 9185993]

84. Arnoczky SP, Warren RF. Microvasculature of the human meniscus. Am J Sports Med. 1936; 10(2):90–5.

85. Han WM, Heo S-J, Driscoll TP, Delucca JF, McLeod CM, Smith LJ, et al. Microstructural heterogeneity directs micromechanics and mechanobiology in native and engineered fibrocartilage. Nat Mater. 2016 Jan.

86. Mikic B, Johnson TL, Chhabra a B, Schalet BJ, Wong M, Hunziker EB. Differential effects of embryonic immobilization on the development of fibrocartilaginous skeletal elements. J Rehabil Res Dev. 2000; 37(2):127–33. [PubMed: 10850818]

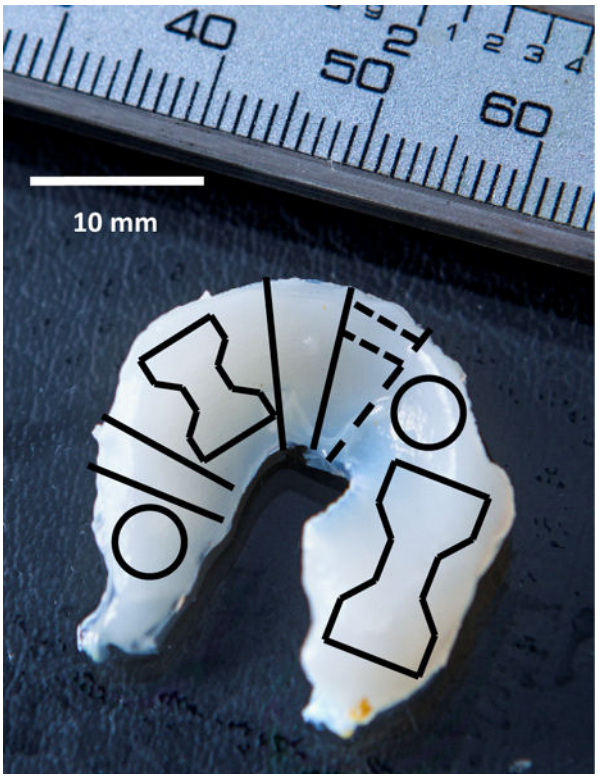

Figure 1.
Sample delegation from constructs at the conclusion of culture. Dogbone shapes were allocated for tensile testing. Circular shapes indicate 4 mm punch biopsies used for compression testing. Solid lines depict cut lines for confocal slices that were also used for histology. Dotted line indicates freeze fracture lines performed on dried SEM samples prior to mounting on SEM stubs. Remaining material was divided into four parts and analyzed for biochemical analysis. Scale bar = 10mm.

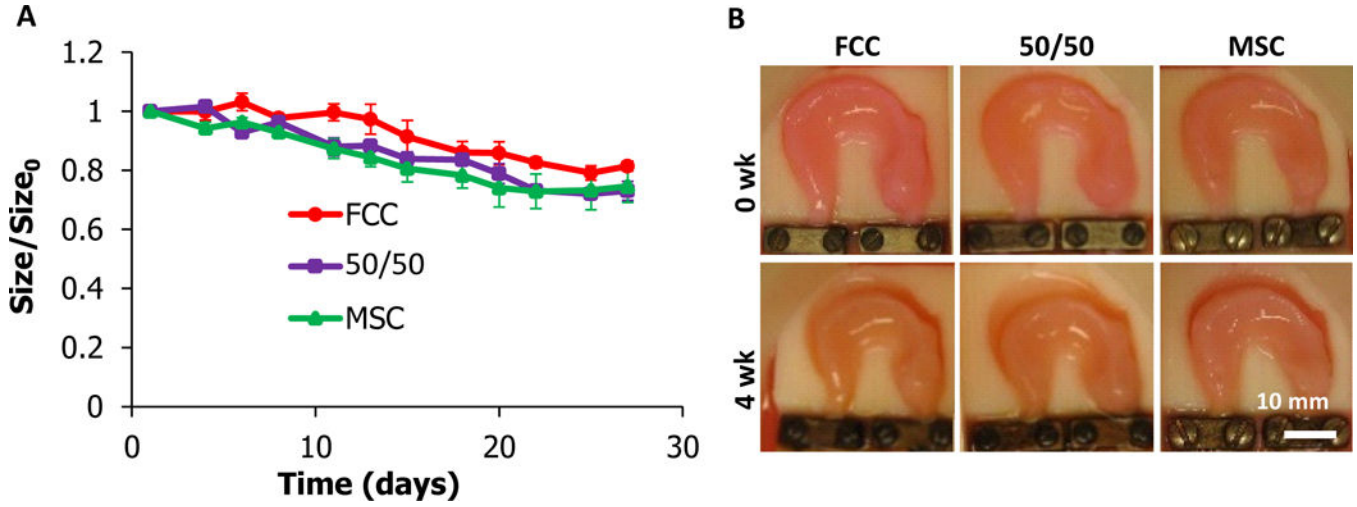

Figure 2.

Tissue engineered meniscal contraction. (A) Ratio of projected area over initial projected area calculations at day 1. (B) Representative images of menisci at 0-, 4- weeks. No statistical difference was observed between culture groups (mean ±SD, n=4, $p<0.05$). scale bar = 10mm.

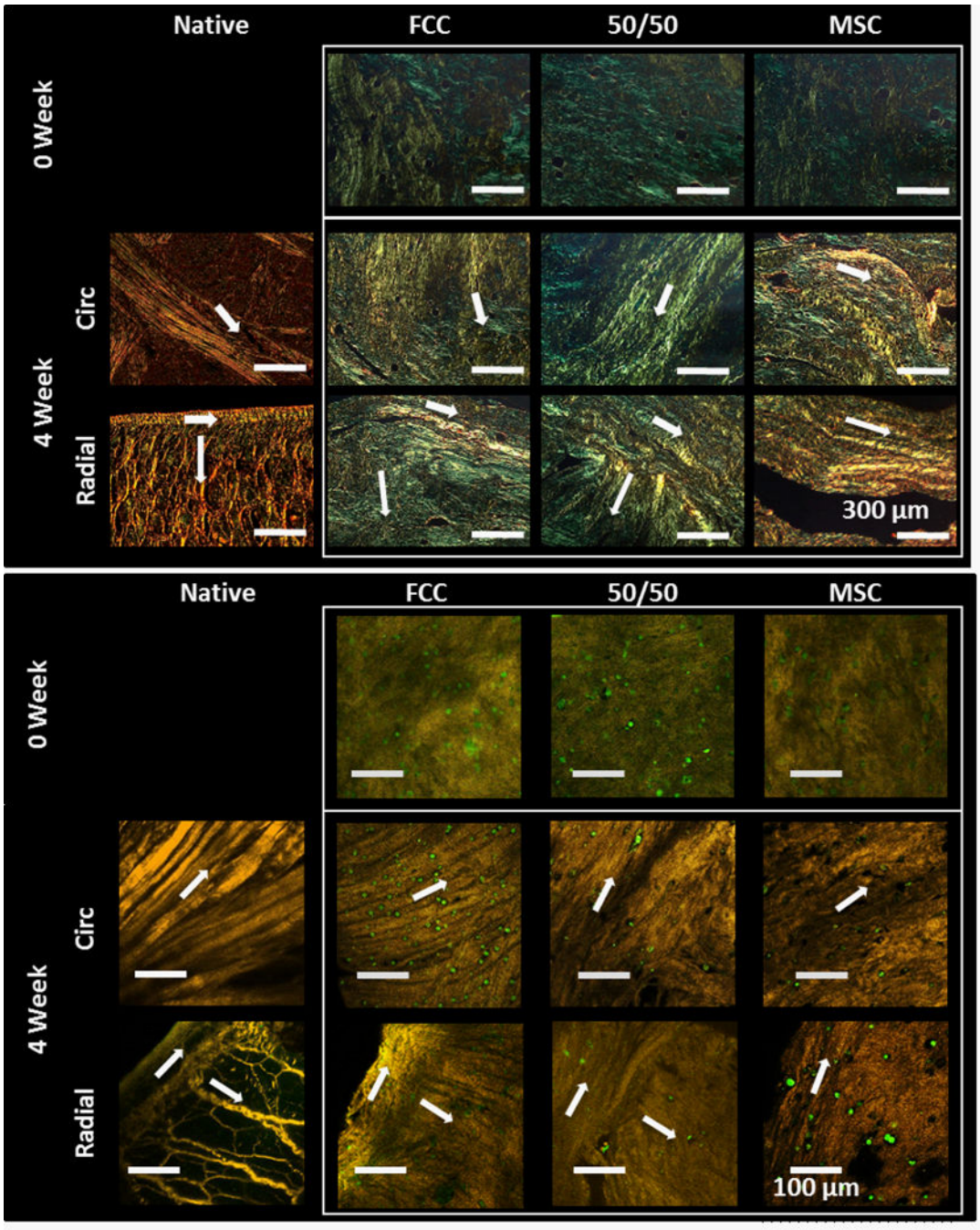

Figure 3.

MSCs and FCCs form fibers in both the circumferential and radial direction (↑ indicates fiber direction). 0 week menisci have mostly small disorganized fibers. After 4 weeks all culture groups have organized fibers with directionality. Circumferential fibers have formed running from horn to horn of menisci. Aligned fibers around the outer edge and extending into the center of the meniscus are visible in the radial direction. (top) Polarized light, scale bar = 300 µm (bottom) SHG with FCCs labeled red and MSCs labeled green, scale bar = 100 µm.

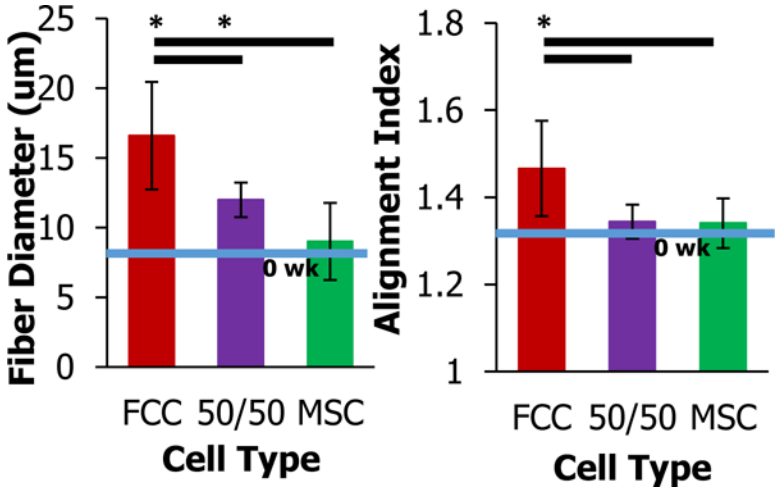

Figure 4.

Fiber diameter and alignment index of circumferential sections at four weeks measured using SHG images analyzed using custom MATLAB code (— significantly different between groups, * significantly different with time, $p<0.05$, n=6-8, 7 images per samples).

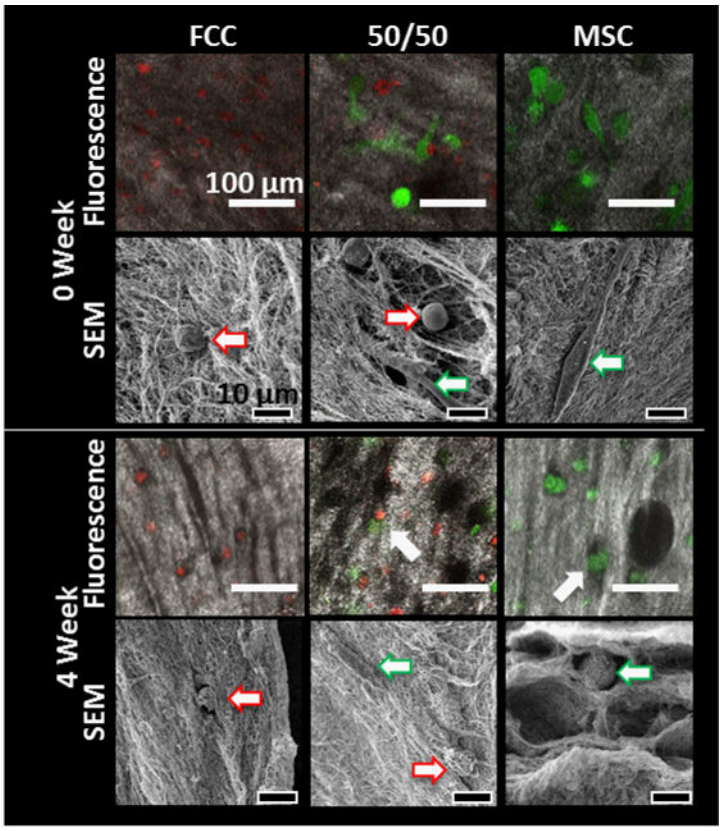

Figure 5.

Fluorescence and scanning electron microscopy (SEM) of cells in collagen gels. Fluorescence images show FCCs in red and MSCs in green with collagen visualized using second harmonic generation (SHG), scale bar = 100 µm. High magnification cell images are taken using SEM, scale bar = 10 µm. MSCs (⟶) shifted to a circular phenotype. FCCs (⟶) integrated into collagen fibers while MSCs (⟶) settled into collagen pores.

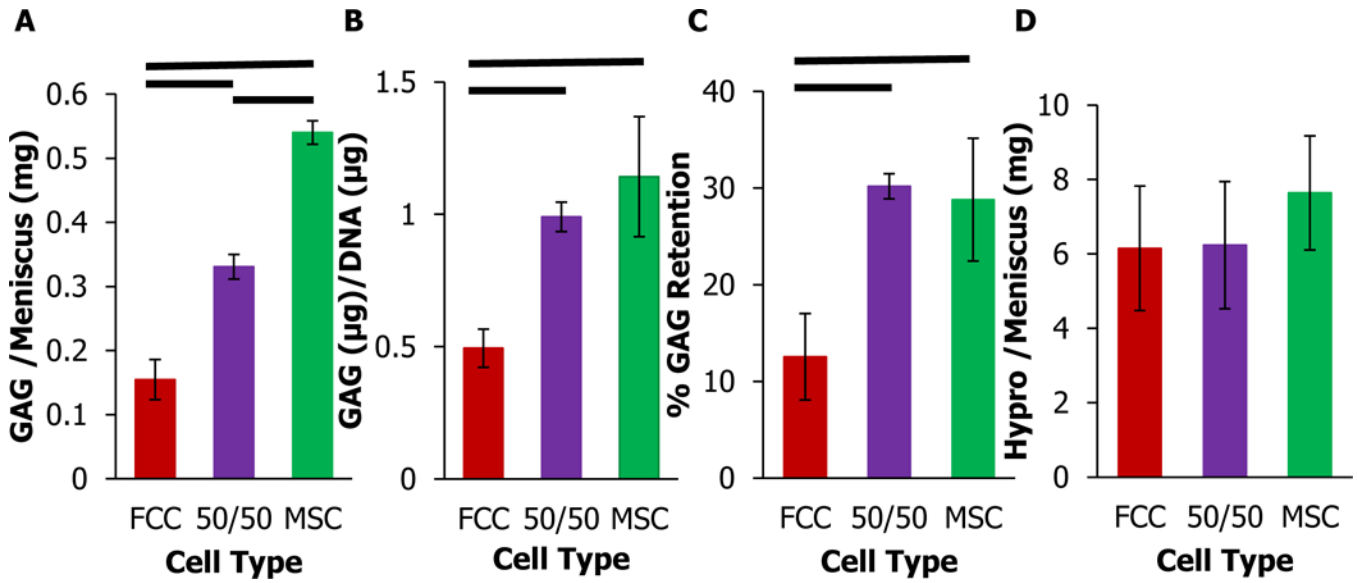

Figure 6.

Biochemical analysis of meniscal constructs at four weeks. (A) Total GAG content per meniscus. (B) GAG normalized to DNA content. (C) % GAG retained in meniscal construct relative to GAG released in media. (D) Hydroxyproline content per meniscus. — significantly different between groups ($p<0.05$, $n=4$).

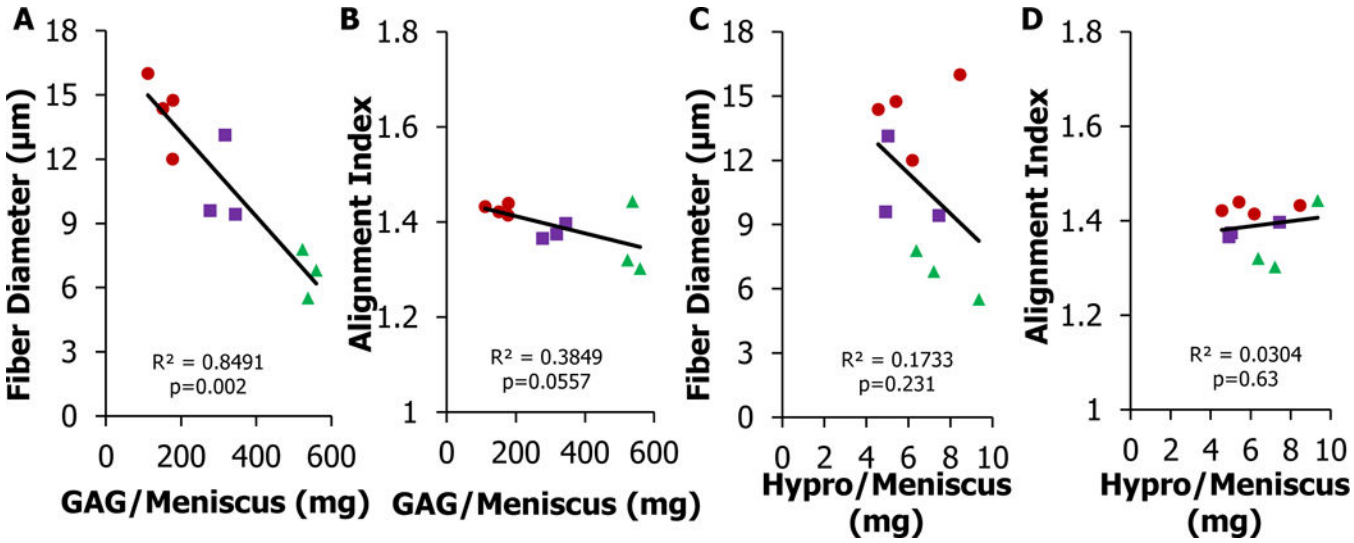

Figure 7.

Fiber formation and biochemical content relationship in tissue engineered menisci (A-B) Total GAG content per meniscus compared to fiber diameter and alignment index. (C-D) Total Hypro content per meniscus compared to fiber diameter and alignment index. Fiber diameter is strongly correlated to GAG/Meniscus ($p<0.05$, $R^2>0.80$). <R> ● FCC, <B> □ 50/50, <G> Δ MSC.

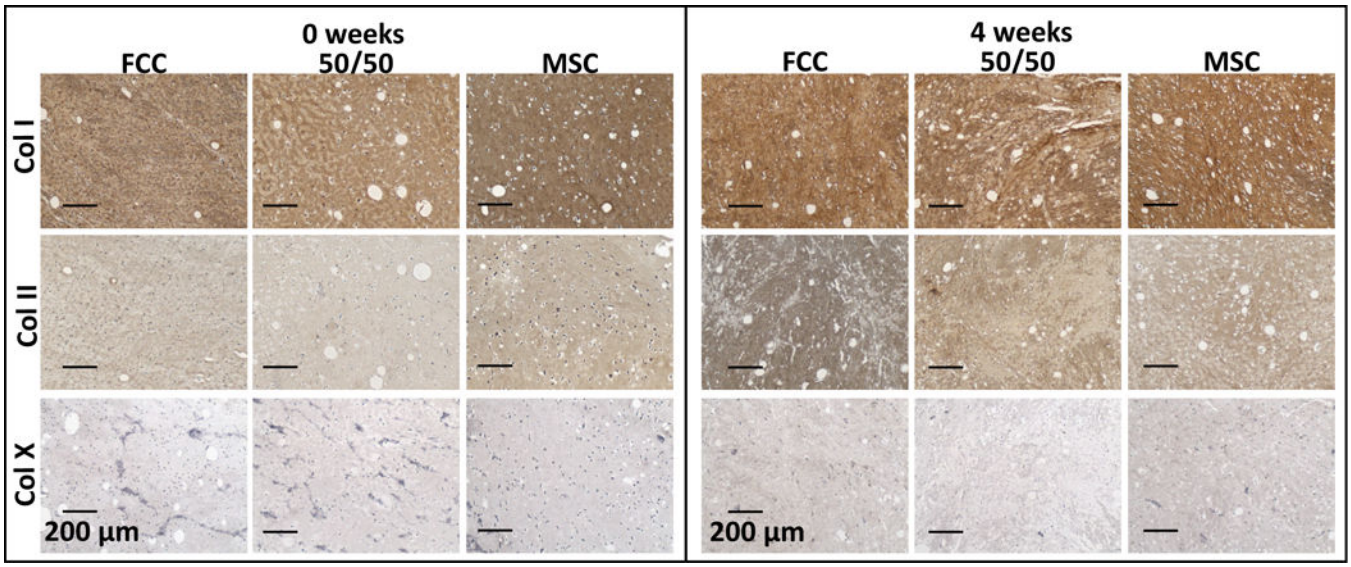

Figure 8.
Immunohistochemical staining for collagen type I, II, and X after 0 and 4 weeks in culture (scale bar=200 µm).